

The unusually large population of Blazhko variables in the globular cluster NGC 5024 (M53)^{*}

A. Arellano Ferro^{1†}, D.M. Bramich^{2‡}, R. Figuera Jaimes^{1§}, Sunetra Giridhar^{3¶},
K. Kuppuswamy^{3||}

¹*Instituto de Astronomía, Universidad Nacional Autónoma de México*

²*European Southern Observatory, Karl-Schwarzschild-Straße 2, 85748 Garching bei München, Germany*

³*Indian Institute of Astrophysics, Koramangala 560034, Bangalore, India*

Accepted . Received ; in original form

ABSTRACT

We report the discovery of amplitude and phase modulations typical of the Blazhko effect in 22 RRc and 9 RRab type RR Lyrae stars in NGC 5024 (M53). This brings the confirmed Blazhko variables in this cluster to 23 RRc and 11 RRab, that represent 66% and 37% of the total population of RRc and RRab stars in the cluster respectively, making NGC 5024 the globular cluster with the largest presently known population of Blazhko RRc stars. We place a lower limit on the overall incidence rate of the Blazhko effect among the RR Lyrae population in this cluster of 52%. New data have allowed us to refine the pulsation periods. The limitations imposed by the time span and sampling of our data prevents reliable estimations of the modulation periods. The amplitudes of the modulations range between 0.02 and 0.39 mag. The RRab and RRc are neatly separated in the CMD, and the RRc Blazhko variables are on average redder than their stable counterparts; these two facts may support the hypothesis that the HB evolution in this cluster is towards the red and that the Blazhko modulations in the RRc stars are connected with the pulsation mode switch.

Key words: Globular Clusters: NGC 5024 – Variable Stars: RR Lyrae, Blazhko effect.

1 INTRODUCTION

In 1907, S. Blažko described the cyclic variation of the pulsation period of RW Dra, without comments on the amplitude behaviour, (Blažko 1907), and in 1916, H. Shapley reported cyclic variations in the shape of the light curve, period and amplitude in the star RR Lyrae (Shapley 1916). Period oscillation and/or amplitude modulation in RR Lyrae type stars is generally referred to as the Blažko or Blazhko effect. Over the last hundred years numerous RR Lyrae stars have been found to exhibit cyclic modulations of both period and amplitude although cases of amplitude modulations with no period variations are common. The cause of these modulations has remained unsatisfactorily explained on theoretical grounds. This is not surprising since, to detect and characterize the variations, even

in the cases with large amplitude modulations, large sets of accurate photometric observations obtained over a long time span are required. Most recently, as a result of careful inspection of large data bases (e.g. Moskalik & Poretti et al. 2003 (OGLE); Kolenberg et al. 2010 (*Kepler*)), the detection of the Blazhko effect in RR Lyrae stars has improved. Long term surveys have proven useful in the detection of very small amplitude modulations, increasing the fraction of known Blazhko variables among the fundamental pulsators RRab (RR0) to about 50% (e.g. the Konkoly Blazhko Survey; Jurcsik et al. 2009) and have also allowed detailed studies of individual objects (e.g. Chadid et al. 2010a (V1127 Aql); Chadid et al. 2010b (S Arae); Poretti et al. 2010 (CoRoT 101128793); Kolenberg et al. 2011 (RR Lyr)).

While knowledge of the Blazhko population in globular clusters would yield important insight to the metallicity influence on the incidence of the Blazhko phenomenon, the study of Blazhko variables in globular clusters is still very much unexploited. Several difficulties including that stars are faint and often in very crowded fields mean that long time series of high quality CCD images and photometry of exceptional high quality are required.

During the course of an investigation into the variable stars in

^{*} Based on observations collected at the Indian Astrophysical Observatory, Hanle, India.

[†] E-mail: armando@astro.unam.mx

[‡] E-mail: dan.bramich@hotmail.co.uk

[§] E-mail: rfiguera@astro.unam.mx

[¶] E-mail: giridhar@iia.res.in

^{||} E-mail: kuppuswamy@iia.res.in

Table 1. Time-series V and I photometry for all the RR Lyrae stars in our field of view. The standard M_{std} and instrumental m_{ins} magnitudes are listed in columns 4 and 5, respectively, corresponding to the variable star, filter, and epoch of mid-exposure listed in columns 1-3, respectively. The uncertainty on m_{ins} is listed in column 6, which also corresponds to the uncertainty on M_{std} . For completeness, we also list the quantities f_{ref} , f_{diff} and p (see Eq. 1 in Paper I) in columns 7, 9 and 11, along with the uncertainties σ_{ref} and σ_{diff} in columns 8 and 10. This is an extract from the full table, which is available with the electronic version of the article (see Supporting Information).

Variable Star ID	Filter	HJD (d)	M_{std} (mag)	m_{ins} (mag)	σ_m (mag)	f_{ref} (ADU s $^{-1}$)	σ_{ref} (ADU s $^{-1}$)	f_{diff} (ADU s $^{-1}$)	σ_{diff} (ADU s $^{-1}$)	p
V1	V	2454939.20002	17.167	18.487	0.003	661.567	1.722	-299.031	1.098	1.1564
V1	V	2454939.23093	17.187	18.507	0.003	661.567	1.722	-309.195	1.076	1.1625
⋮	⋮	⋮	⋮	⋮	⋮	⋮	⋮	⋮	⋮	⋮
V1	I	2454939.19220	16.541	17.935	0.003	782.781	3.855	-134.485	2.042	1.1907
V1	I	2454939.20744	16.528	17.922	0.003	782.781	3.855	-122.903	1.961	1.1757
⋮	⋮	⋮	⋮	⋮	⋮	⋮	⋮	⋮	⋮	⋮

the globular cluster NGC 5024 (M53) based on V and I CCD photometry (Arellano Ferro et al. 2011; Paper I), clear amplitude and light curve shape variations were detected in a few RRab stars and in the majority of the RRc stars. These Blazhko-like variations are surprising since the Blazhko effect has been mostly associated with RRab stars and not so much with RRc stars. Amplitude and phase modulations were found in RRc stars only recently in three stars in M55 (namely V9, V10 and V12) (Olech et al. 1999), in the LMC (2-4% of the RRc stars) (Alcock et al. 2000), in NGC 6362 (namely V6, V10 and V37) (Olech et al. 2001) and in three RRc stars in the OGLE database (BWC V47, MM5A V20 and BW8 V34) (Moskalik & Poretti 2003). In these stars, non-radial modes with very close frequencies to the primary frequency have been identified and the beating of these pulsational modes results in long-term amplitude and phase modulations. A different scenario is that the modulation produces asymmetric sidepeaks to the primary but that due to limited accuracy of ground-based data one only sees the most prominent peaks (Benkő et al. 2010). However, in higher accuracy space-based data, such as from the CoRoT and Kepler missions, the full spectrum of side peaks is always visible irrespective of what the cause of the modulations might be.

In this paper we present the detection of Blazhko-type amplitude and phase modulation in the majority of RRab and RRc variables in the globular cluster NGC 5024. Despite the limited time span of our data and of the sparse coverage of the modulation cycle, we have made an attempt to estimate the modulation period, which we find to be reliable only in a few cases.

The globular cluster NGC 5024 (M53) (R.A.(2000)13^h12^m55^s.3, DEC(2000)= +18°10′09″) is located in the intermediate galactic halo ($l=332.97$, $b=+79.77$, $Z = 17.5$ kpc, $R_G=18.3$ kpc and as a consequence it is subject to very low reddening ($E(B - V) = 0.02$). Its metallicity $[\text{Fe}/\text{H}] \sim -1.92 \pm 0.06$ and an average distance $d \sim 18.3 \pm 0.4$ kpc have been calculated from the RR Lyrae stars in Paper I.

2 OBSERVATIONS AND REDUCTIONS

We have complemented the observations reported in Paper I with new Johnson V and I observations obtained on March 12 and 13, and April 11, 12, 13 and 14, 2011. The observations were performed with the 2.0m telescope of the Indian Astronomical Observatory (IAO), Hanle, India, located at 4500m above sea level. The estimated seeing was ~ 1 arcsec. The detector was a Thompson CCD of 2048×2048 pixels with a pixel scale of 0.296 arc-

sec/pix and a field of view of approximately 10.1×10.1 arcmin 2 . The new observations have brought the number of available epochs from 177 in the V -band and 184 in the I -band in Paper I, to 297 and 307 in V and I respectively. As in Paper I, we employed the technique of difference image analysis (DIA) to extract high precision photometry for all point sources in the images of NGC 5024 (Alard & Lupton 1998; Alard 2000; Bramich et al. 2005). We used a pre-release version of the DanDIA¹ pipeline for the data reduction process (Bramich et al., in preparation) which includes a new algorithm that models the convolution kernel matching the point-spread function (PSF) of a pair of images of the same field as a discrete pixel array (Bramich 2008). The transformations to the standard system were as discussed in Paper I. For the sake of homogeneity we choose to use the same transformation equations calculated in Paper I to transform the new set of data to the standard Johnson-Kron-Cousins photometric system. All our new V , I photometry for the variables in the field of our images for NGC 5024 is reported in Table 1. For the sake of commodity to the interested reader we have also included in the table the V , I data from Paper I supplemented by the new observations. The parameters f_{ref} , f_{diff} and p are fundamental to the difference imaging method and allow to reconstruct the original fluxes on the images, hence they are included in Table 1. Their exact definitions are given in Paper I (section 2) and the interested reader is referred to that paper. Only a small portion of Table 1 is given in the printed version of this paper but the full table is available in electronic form.

3 PULSATION PERIODS

We have applied the string-length method (Burke et al. 1970; Dworetzky 1983) to the light curves which determines the best period and a corresponding normalized string-length statistic S_Q to estimate the pulsation periods of all the RR Lyrae stars in our sample. The so determined periods and the epochs employed to phase the light curves are listed in Table 2.

4 LIGHT CURVES OF THE RR LYRAE STARS

The V light curves of the RRab and RRc stars, phased with the ephemerides in Table 2, are displayed in Figs. 1 and 2. The phase

¹ DanDIA is built from the DanIDL library of IDL routines available at <http://www.danidl.co.uk>

Table 2. Periods and epochs of the RR Lyrae stars in NGC 5024 in our field of view.

Variable	Bailey's type	P (days)	HJD _{max} (+240 0000.)	Variable	Bailey's type	P (days)	HJD _{max} (+240 0000.)
V1	RRab	0.609823	55633.427	V38	RRab-BI	0.705793	55220.482
V2	RRc-BI	0.386146	54940.342	V40	RRc	0.314820	55264.433
V3	RRab	0.630596	55633.450	V41	RRab-BI	0.614440	55323.107
V4	RRc-BI	0.385609	55666.170	V42	RRab	0.713716	55665.270
V5	RRab	0.639425	55249.474	V43	RRab-BI	0.712014	54941.204
V6	RRab	0.664019	55294.248	V44	RRc-BI	0.374908	55666.237
V7	RRab	0.544860	54940.391	V45	RRab	0.654944	55633.439
V8	RRab	0.615524	55666.180	V46	RRab-BI	0.703649	55665.230
V9	RRab	0.600371	55633.411	V47	RRc-BI	0.335366	55249.380
V10	RRab	0.608267	55665.264	V51	RRc-BI	0.355215	55663.253
V11	RRab-BI	0.629946	55665.270	V52	RRc-BI ^a	0.364621	55666.242
V15	RRc-BI	0.308692	55666.242	V53	RRc-BI ^a	0.389080	55633.411
V16	RRc-BI	0.303160	55294.257	V54	RRc-BI	0.315107	55664.379
V17	RRc-BI	0.381098	55323.183	V55	RRc-BI	0.443227	55666.252
V18	RRc-BI	0.336060	55666.242	V56	RRc	0.328894	55220.457
V19	RRc	0.391159	55633.387	V57	RRab-BI	0.568244	55633.379
V23	RRc-BI	0.366141	54940.391	V58	RRc-BI	0.354971	55663.244
V24	RRab	0.763201	55666.229	V59	RRc-BI	0.303942	55664.334
V25	RRab-BI	0.705153	55264.341	V60	RRab-BI	0.644756	55633.368
V27	RRab	0.671067	54940.342	V61	RRc-BI	0.369930	54940.176
V29	RRab-BI	0.823249	55634.507	V62	RRc-BI	0.359887	55663.261
V31	RRab-BI	0.705670	55634.386	V63	RRc-BI	0.310466	55634.403
V32	RRc-BI	0.390076	55634.393	V64	RRc-BI	0.319724	55634.378
V33	RRab-BI	0.624589	54941.416	V71	RRc	0.304509	54939.249
V34	RRc	0.289625	54941.266	V72	RRc	0.340749	55664.370
V35	RRc-BI	0.372668	55264.280	V91	RRc	0.302426	55634.474
V36	RRc-BI	0.373301	54941.430	V92	RRc	0.277222	55633.509
V37	RRab	0.717617	55663.249				

BI: Blazhko variables with the S_B -index larger than 145. *a*: V52 and V53 lie in close spatial proximity and it is possible that flux contamination between the variables is, at least a partial cause of the observed Blazhko effect.

coverage is very good in all cases. Different colours and symbols have been used to highlight the nightly variations of the light curve shape. The date-colour code is listed in Table 3. The night of January 22 (JD 2455219.) only contains two data points, hence it was neither coded nor plotted.

Amplitude and phase modulations are clearly visible in the light curves for most stars. Light curves without visible evidence of modulations have been plotted with black symbols and it can be argued that the stability of these stars helps in proving that the modulations detected in the rest of the stars are real and not an artifact of our reductions. Further insight on the stability of the reduction process will be addressed in section 5.1.

The light curves in the I -band have been carefully explored and despite having smaller amplitude variations than in the V -band, and hence smaller Blazhko modulations, the effect is very obvious and consistent with the V band counterparts. For the sake of brevity, we do not plot the I light curves but the data are included in Table 1.

5 RR LYRAE STARS WITH THE BLAZHKO EFFECT

RR Lyrae stars exhibiting the Blazhko effect in NGC 5024 have been reported by Dékány & Kovács (2009); two RRab stars, V11 and V57, and one RRc star, V16. The corresponding light curves in Fig. 1 and 2 indeed exhibit clear signs of the amplitude modulation. We have noticed amplitude and light curve shape variations in the majority of the RRc and in a number of other RRab stars.

The appearance of the light curves in most RRc stars resembles the light curves of the amplitude modulated RRc stars found by Olech et al. (1999) in M55. Clear amplitude changes are observed over time scales of days. In order to make the time variations of the light curves more evident, in Figs. 3 and 4 we plot the residuals of the phased light curves relative to a fitted Fourier model (see Paper I; fits are redone including the new photometric data) following the same colour code in Table 3. These plots highlight the amplitude variation scale and help to distinguish small, rather marginal, amplitude modulations.

We inspected each star in the reference image looking for blends or other possible defects that may cause systematic errors in the overall light curve amplitudes. A blended reference flux will not change the shape of the light curve but it will affect the amplitude (see Bramich et al. 2011 for a more detailed discussion). Hence, any Blazhko variations will exhibit exactly the same form regardless of the reference flux, but the measured amplitudes of these excursions from the mean curve may be affected. Then, it is convenient to note the location of each variable in the general field of the cluster. We offer a guide of the level of blending by defining the “inner” and the “outer” regions of the cluster. Any star in the central region of the cluster is most likely blended with fainter stars whereas in the outer region this problem is negligible. Despite the good PSF subtraction of most stars in the cluster when measuring the reference fluxes on the reference image, in the central region the systematic residuals are always more prominent than in the outer region. An examination of the residuals of the reference image suggests as a reasonable border-line a circle of radius 60 arcsec centred on the cluster. In the

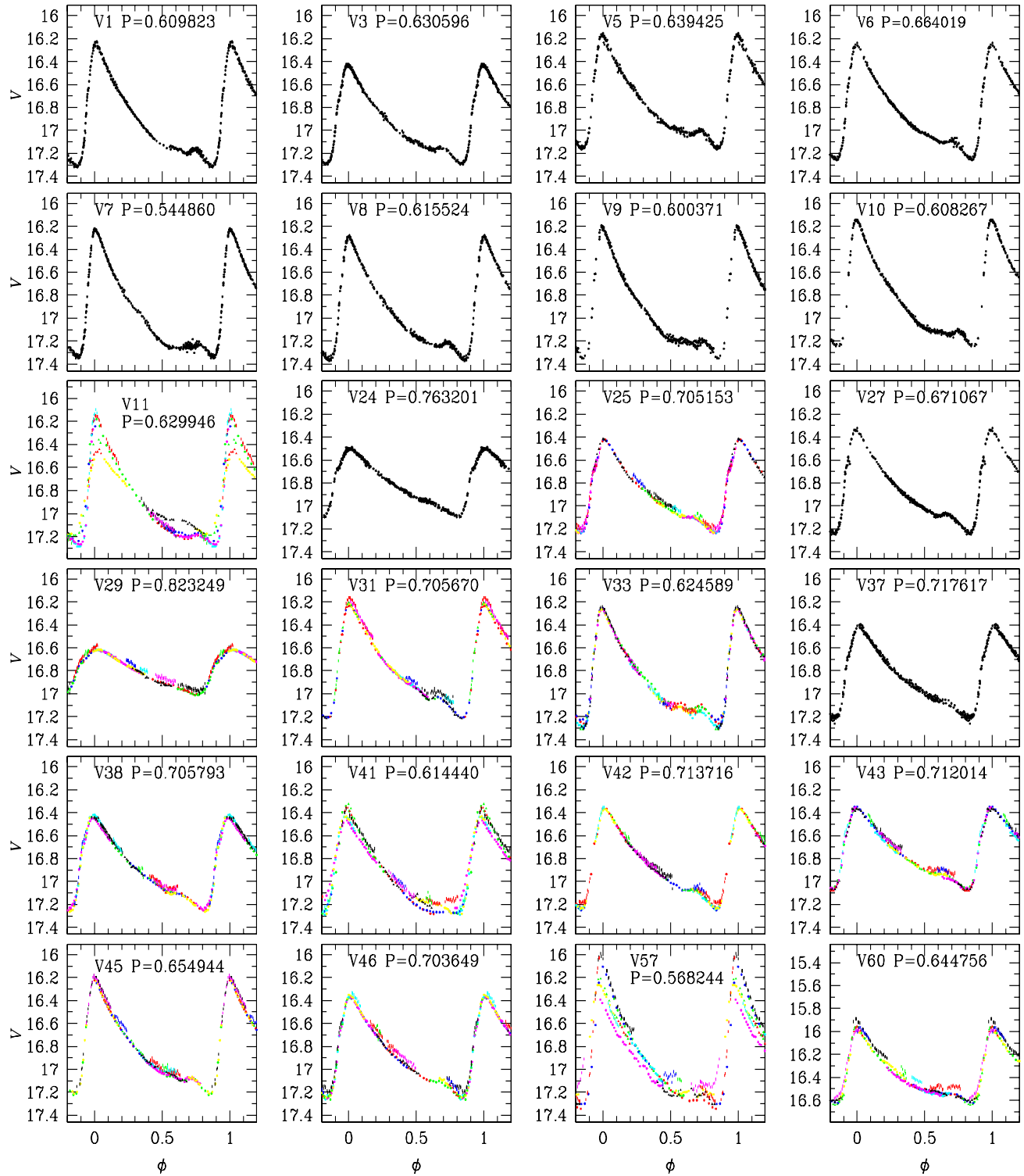


Figure 1. Phased V light curves of the RRab stars. For stars showing signs of amplitude and phase modulations, different colours have been used for individual nights following the code given in Table 3. Stars for which the light curves are seemingly non-modulated are displayed with black dots and give a sense of the reliability of our photometry.

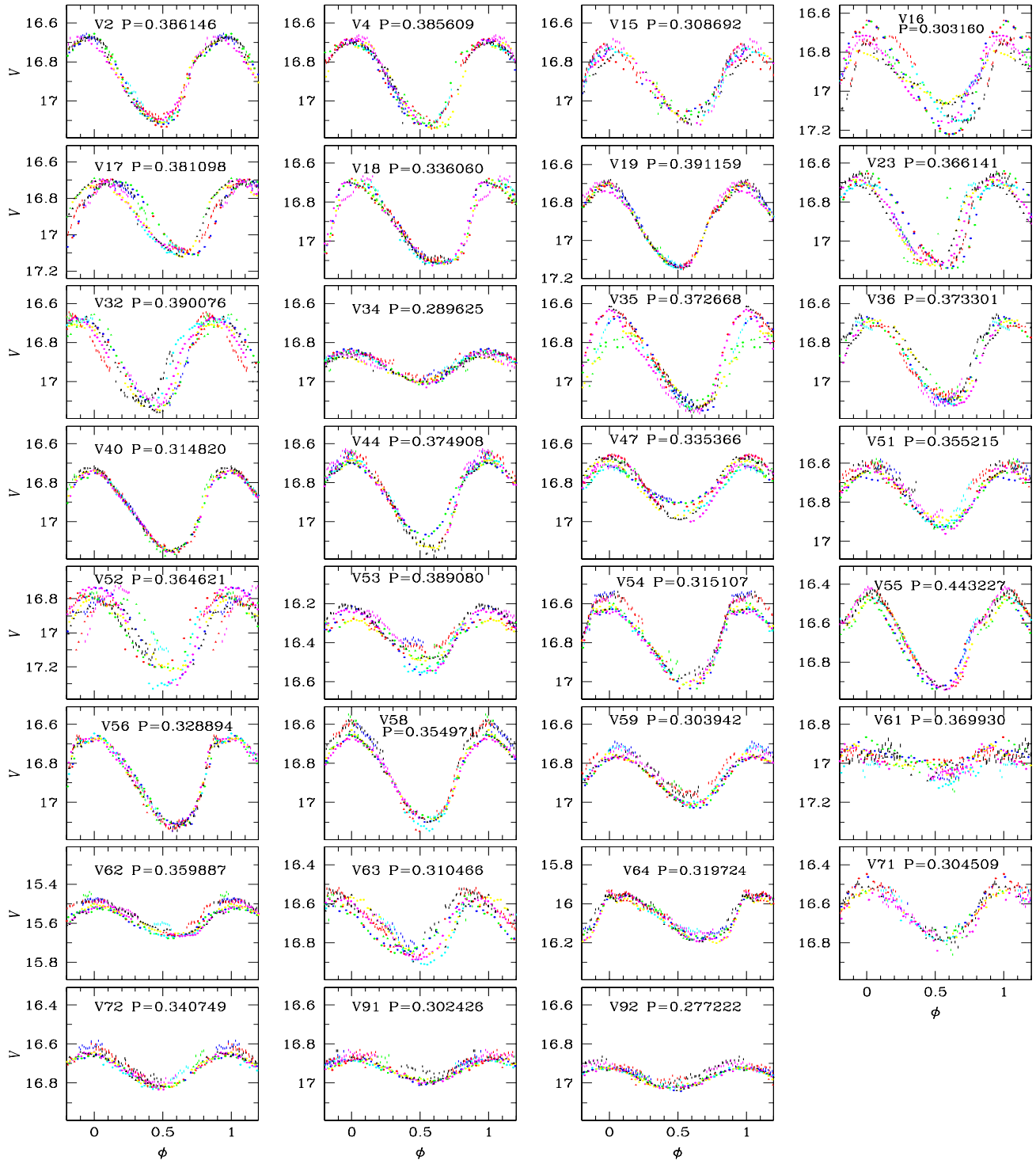


Figure 2. Phased V light curves of the RRc stars. The colour-code for the symbols is the same as in Fig. 1 (as defined in Table 3).

comments column of Tables 4 and 5, we indicate to which region each star belongs and the extent of any blending. While the brightness of some stars is indeed very likely contaminated by nearby stars, some others are comfortably isolated. We decided to retain the complete sample for further evaluation.

At this stage, we deem it necessary to demonstrate that the

observed amplitude and phase modulations of the RR Lyrae stars in NGC 5024 are not caused by inaccuracies in our observations and/or systematic errors introduced by our reduction software. The following subsections deal with this aspect.

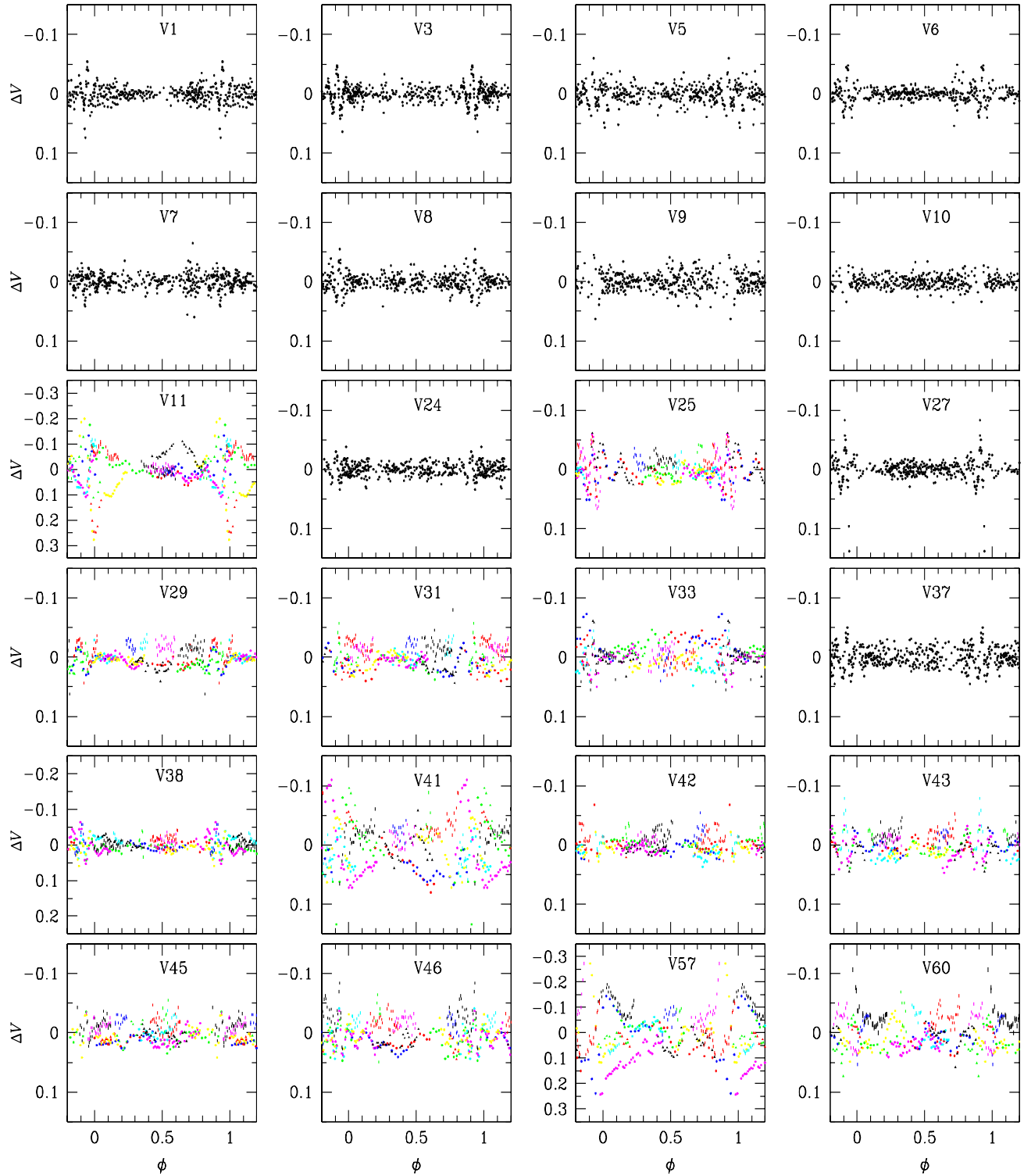


Figure 3. Residuals of the V phased light curves relative to a fitted Fourier model for the RRab stars. Systematic nightly differences relative to the model light variation can be clearly observed in most variables which we interpret as due to the Blazhko amplitude and/or phase modulation. See the text for a discussion on individual cases. The colour code is as in Fig. 1. Note that the vertical scale is different for a few stars with the largest amplitude modulations (V11, V38 and V57). Typical photometric uncertainty is 0.008 mag.

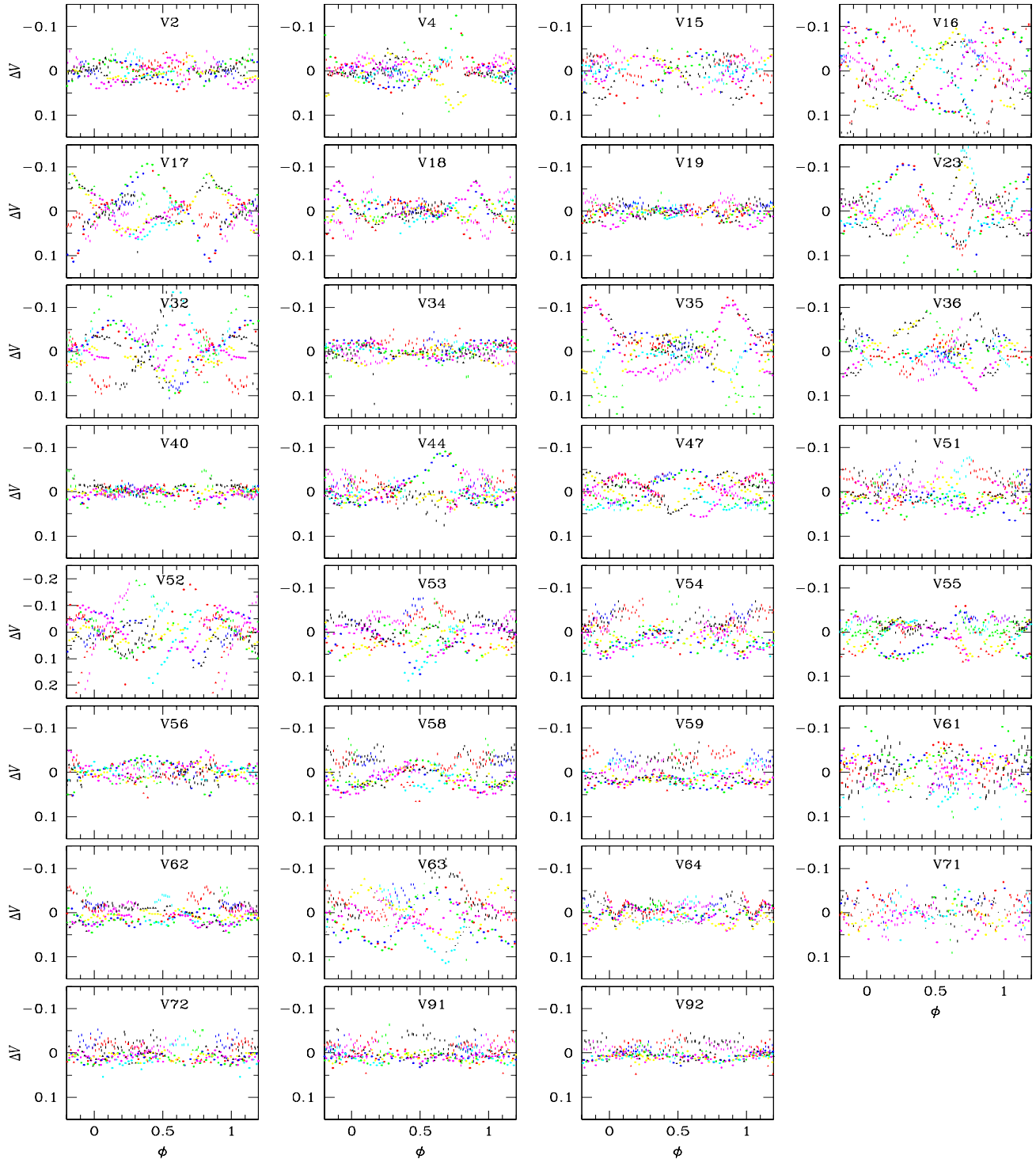


Figure 4. Residuals of the V phased light curves relative to a fitted Fourier model for the RRc stars. See also the caption to Fig. 3.

5.1 Analysis of systematic errors in the photometry

In this section we attempt to disentangle the systematic errors caused during the `DanDIA` reduction process from the genuine “Blazhko” variations. Our approach consists of generate simulated time-series calibrated imaging data that contains simulated RR Lyrae variables with perfectly stable model light curves (i.e. no

Blazhko effect), and then reducing the simulated imaging data with the `DanDIA` pipeline. The extracted light curves of the simulated RR Lyrae stars will then allow an assessment of the level to which systematic errors in the reductions can imitate the Blazhko effect. Note that we only consider the V filter in this analysis because this

Table 3. Julian date colour-code used in Figs. 1, 2, 3, 4 and 5.

HJD (d)	Colour
245 4939.	red circles
245 4940.	green circles
245 4941.	blue circles
245 5220.	turquoise circles
245 5249.	purple circles
245 5263.	yellow circles
245 5264.	black triangles
245 5294.	red triangles
245 5323.	green triangles
245 5633.	black tick
245 5634.	red tick
245 5663.	green tick
245 5664.	blue tick
245 5665.	turquoise tick
245 5666.	purple tick

is the waveband in which the Blazhko effect has the greatest photometric amplitude.

5.1.1 Simulating images of NGC 5024

The reductions of the real imaging data of NGC 5024 provide us with all the information we require to generate a set of time-series model calibrated images for the cluster. By taking the extra step of adding noise to the model image pixel values using the adopted noise model for the CCD, we may generate a set of realistic simulated observations of the cluster closely matching the properties of our real calibrated imaging data.

We start with the list of 9075 stars detected on the reference image for the *V* filter, adopting their detected positions and measured reference fluxes as model values. Included in this list are the 24 RR0 and 31 RR1 variable stars in NGC 5024 for which we have real light curve data. For each of these variable stars, we adopt the fitted Fourier decomposition of the phased light curve as the model light curve, which we convert to flux units on the reference image using the model reference flux. For all the remaining stars, we assume that they are non-variables, and we adopt a model light curve consisting of a constant flux on the reference image equal to the model reference flux.

For each real image in our time-series imaging data, we carry out the following procedure to generate a corresponding simulated calibrated image of the cluster:

- (i) We create a model image array with the same dimensions as a real calibrated image such that each pixel value is equal to the measured sky level (ADU) in the current real image.
- (ii) We calculate the model flux of each star at the epoch corresponding to the current real image using its model light curve, and we then adjust this flux by multiplying by the photometric scale factor derived for the real image during the image subtraction stage of DanDIA. This yields a model flux (ADU) for each star on the flux scale of the current real image.
- (iii) We calculate the pixel coordinates of each star in the model image by transforming the reference-image pixel-coordinates using the coordinate transformation derived between the reference image and the current real image during the image registration stage of DanDIA.
- (iv) For each star, we generate a model PSF on the model image

using the following method. We calculate the star PSF on the reference image by evaluating the reference-image model-PSF from the DanDIA reductions at the reference-image pixel-coordinates of the star. The reference-image model-PSF corresponds to the pixel centres, and it is therefore necessary to shift the star PSF with a sub-pixel shift (via cubic O-MOMS resampling, see Blu et al. 2001) so as to match the subpixel coordinates of the star in the model image. Since any rotation, shear or scale change between the real images in our time-series is negligible, no further coordinate transformation of the star PSF is necessary. We then convolve the star PSF with the kernel solution for the current real image from the DanDIA reductions evaluated at the reference-image pixel-coordinates of the star. Finally, we enforce the star PSF normalisation to a sum of unity.

(v) For each star, we add the model PSF generated in step (iv) scaled by the corresponding model flux calculated in step (ii) to the model image created in step (i) at the star’s pixel coordinates calculated in step (iii). This results in the production of a model calibrated image corresponding to the current real image.

(vi) For each pixel in the model image, indexed by column i and row j , we calculate the following noise map σ_{ij} using the standard CCD noise model for calibrated images adopted by the DanDIA software:

$$\sigma_{ij} = \sqrt{\frac{\sigma_0^2}{F_{ij}^2} + \frac{M_{ij}}{GF_{ij}}} \quad (1)$$

where $\sigma_0 = 6.5$ ADU is the CCD readout noise, $G = 1.3 \text{ e}^-/\text{ADU}$ is the CCD gain, F_{ij} is the master flat-field image used to calibrate the current real image, and M_{ij} is the model image we have generated in step (v) (see Bramich 2008).

(vii) Again, for each pixel in the model image, we generate a random number drawn from a normal distribution with zero mean and unit sigma, multiply these numbers by the noise map σ_{ij} , and add them to the model image from step (v). This results in the production of a simulated noisy calibrated image corresponding to the current real image.

(viii) We use a copy of the bad pixel mask for the current real calibrated image as the bad pixel mask for the simulated calibrated image, which includes bad pixels corresponding to saturated pixels.

We note that saturated stars are not included in the reference-image star-list that is provided by the DanDIA software, and therefore the simulated images generated by the above procedure do not include any flux from saturated stars in the reference image. However, the adoption of the real bad pixel masks for the simulated images ensures that any pixels that could contain flux from a saturated star are properly masked during the reduction process.

5.1.2 Reduction of the simulated images of NGC 5024

We reduced the simulated images generated in Section 5.1.1 using the DanDIA pipeline with exactly the same parameters as those used for reducing our real time-series imaging data. We constructed the simulated reference image from the simulated images corresponding to the real images used to construct the real reference image, and we detected 8982 stars on the simulated reference image from the 9075 real star records that were used to generate the simulated images. The pipeline successfully processed all 297 simulated images, and extracted light curves for 8923 stars, including a light curve for each of the RR Lyrae variables for which we have real light curve data.

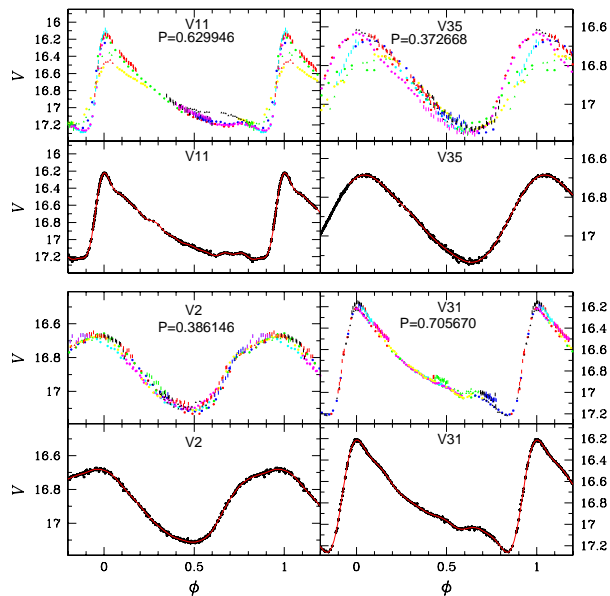


Figure 5. al light curves and their counterparts measured from the simulated images for two clear Blazhko variables (V11 and V35) and two suspected cases (V2 and V31). The stability of the light curves extracted from the simulated images demonstrates that the modulations in the observed light curves are real. The red curves represent the fits to the real light curves that were used to generate the variable star fluxes in the simulated images.

5.1.3 Results

In Figure 5, we plot the real phased light curves (upper panel in each case) and the light curves extracted from the simulated images (black points in the lower panel in each case) for two RRAb stars and for two RRC stars. V11 and V35 have very clear Blazhko effects in the real light curves, and V2 and V31 have suspected low-amplitude Blazhko effects. The most striking feature of these plots is how closely the simulated light curves follow the input model light curves (red curves in the lower panel in each case) with what seems to be only random scatter around the input model consistent with the data point uncertainties. To the eye, it is clear that our reduction pipeline has not introduced any systematic errors that could be mistaken as a Blazhko effect, even in the less obvious cases of V2 and V31. This observation is true of all the light curves extracted from the simulated images.

However, to be able to analyse these results more robustly, we must find a way to quantify the amount of Blazhko effect that is present in a phased light curve so that we may quantitatively compare our real light curves with the simulated light curves, and we do this in the next Section.

5.2 A detection statistic for Blazhko modulations

While most Blazhko modulated RR Lyrae variables can be distinguished by a close visual inspection of the phased light curve, the marginal cases may be subject to the personal opinion of the observer. With the aim of quantifying the level of the Blazhko effect present in a light curve, and to provide a numerical method for detecting its presence, we need to develop an appropriate detection statistic. We consider the “alarm” \mathcal{A} statistic designed by Tamuz, Mazeh & North (2006) (see their Section 4 and Equation 3) for the detection of systematic deviations of a light curve from a fitted model. In contrast to the χ^2 goodness-of-fit statistic, the Tamuz \mathcal{A}

statistic takes into account both the size of the residuals and the size of the runs of consecutive residuals of the same sign. Such a statistic is therefore well-adapted to the detection of the Blazhko effect which can be considered as a systematic deviation from a stable perfectly-repeating light curve.

We found that clear Blazhko variables with large amplitude modulations actually produce a low value of the \mathcal{A} statistic, and that non-modulated stars tend to have relatively large \mathcal{A} statistic values. This is contrary to what we expect and to the philosophy of the \mathcal{A} statistic. We traced this problem down to the fact that the \mathcal{A} statistic is normalised by the χ^2 statistic. Blazhko variables with large amplitude modulations have both long consecutive groups of large residuals of the same sign and a large χ^2 value, which cancel out in the calculation of the \mathcal{A} statistic to produce an undesirably low value. We have modified the \mathcal{A} statistic in order to avoid this design flaw by choosing to normalise the statistic by the number of data points rather than by the χ^2 .

We define a new statistic \mathcal{S}_B for the detection of the Blazhko effect as follows:

$$\mathcal{S}_B = \frac{1}{N} \sum_{i=1}^M \left(\frac{r_{i,1}}{\sigma_{i,1}} + \frac{r_{i,2}}{\sigma_{i,2}} + \dots + \frac{r_{i,k_i}}{\sigma_{i,k_i}} \right)^2, \quad (2)$$

where N is the total number of data points in the light curve, and M is the number of groups of time-consecutive residuals of the same sign from a perfectly-repeating light curve model (e.g. a Fourier decomposition fit). The residuals $r_{i,1}$ to r_{i,k_i} form the i th group of k_i time-consecutive residuals of the same sign with corresponding uncertainties $\sigma_{i,1}$ to σ_{i,k_i} . Our Blazhko detection statistic \mathcal{S}_B may therefore be interpreted as a measure of the systematic deviation per data point of the light curve from the perfectly-repeating model.

Fig. 6 shows the values of the \mathcal{S}_B statistic for the real light curves of the RR Lyrae stars plotted against the variable number. Blue and green symbols are used for the RRAb and RRC stars respectively. We also plot the values of the \mathcal{S}_B statistic for the corresponding light curves extracted from the simulated images in Section 5.1.2 as the small black dots. It is clear that the \mathcal{S}_B statistic values are much smaller in general for the simulated light curves when compared to the real light curves, which demonstrates that the observed amplitude and/or phase modulations of the RR Lyrae stars are real, and not an artifact of the reduction process.

The two stars with by far the largest values of the \mathcal{S}_B statistic for the simulated light curves are V52 and V53, which lie in close spatial proximity to each other (see the finding chart in Paper I). Since the *simulated* light curves of these two variables show amplitude and phase variations, it is clear that they are suffering mutual flux contamination during the reduction process. We have ignored these two stars in setting the threshold of the \mathcal{S}_B statistic for Blazhko detection, and instead we set a threshold of $\mathcal{S}_B=145$ just above the \mathcal{S}_B statistic value for the simulated light curve of V57, which has the next largest value. This threshold is plotted in Figure 6 as a horizontal line. We consider that we have detected the Blazhko effect in a real light curve if its corresponding \mathcal{S}_B statistic value is greater than this threshold, and we plot such variables with a triangle symbol. Stars for which we do not detect the Blazhko effect are plotted as circles.

By adopting a threshold for the \mathcal{S}_B statistic that lies above the \mathcal{S}_B statistic values for all of our simulated light curves (with the exception of the special cases of V52 and V53), we are ensuring that we would not erroneously “detect” the Blazhko effect in any of the simulated light curves (a false positive detection). This is important since the values of the \mathcal{S}_B statistic for the simulated light curves include the contribution of the systematic errors introduced

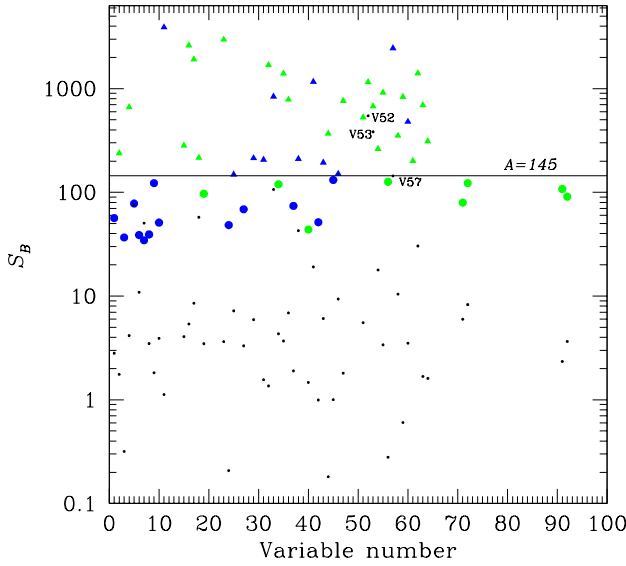


Figure 6. The S_B statistic for all RR Lyrae stars. Blue symbols are for RRab stars, green symbols for RRC stars. Triangles are used for modulated stars and filled circles for non-modulated stars. The value of $S_B=145$ is our adopted threshold line between modulated and non-modulated stars. Small black dots are used for values from the simulated light curves, among which three peculiar cases are labeled: V52, V53 and V57. See text for a discussion.

by our reduction software in our photometry, which will also be present in our real light curves.

On the basis of the above discussions we list in Table 4 the variables in NGC 5024 for which we have detected the Blazhko effect. Stars with $S_B < 145$ are considered to be non-modulated stars within the limits of our data and are listed in Table 5.

Close to the threshold line in Fig. 6 there are some stars whose Blazhko nature will most likely be clarified when more data of good quality and denser sampling become available.

6 DISCUSSION

Globular clusters rich in RR Lyrae stars often have large proportions of Blazhko variables, for example M3 (Smith 1981), M5 (Jurcsik et al. 2011), M68 (Walker 1994), ω Cen (Jurcsik et al. 2001), NGC 362 (Székely et al. 2006) and NGC 3201 (Piersimoni et al. 2002). It has been a generally accepted idea that the Blazhko effect occurred in 20-30% of the RRab stars. However, the analysis of large data sets and detailed studies based on high-quality and long-term data of individual stars, has revealed that the incidence of the Blazhko phenomenon may be as large as 50% in RRab stars, and that amplitude and phase modulations may be present in hitherto unknown cases (e.g Jurcsik et al. 2009, Chadid et al. 2010; Poretti et al. 2010; Benkő et al. 2010).

Most of the above discussions on the incidence of Blazhko variables have principally involved the number of fundamental pulsators (or RRab stars) since the effect in first overtone pulsators (or RRC stars) has been detected only in the last ten years and their number is too small for statistical work. Olech et al. (1999) found

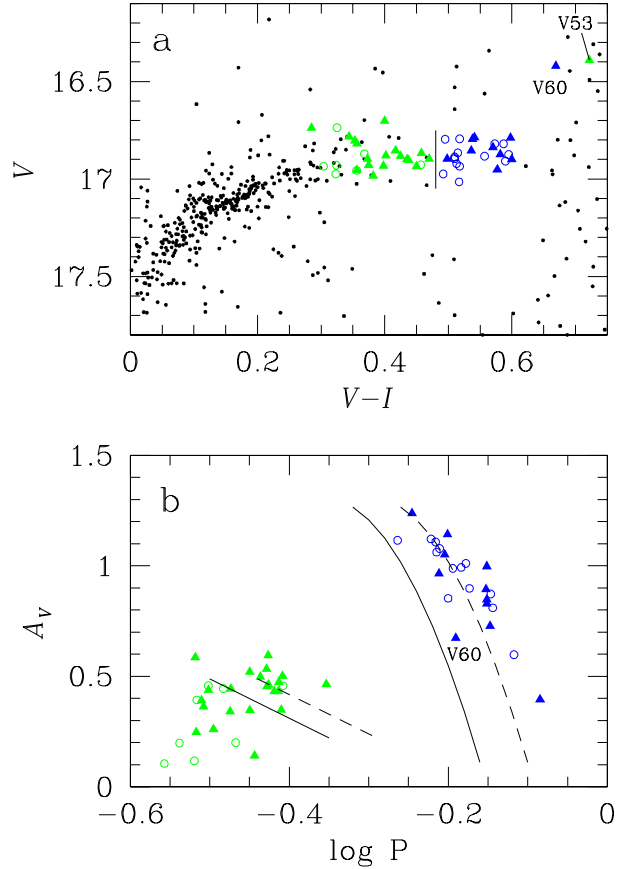


Figure 7. Panel a) shows the distribution of the RR Lyrae stars in the Horizontal Branch. RRC stars are green symbols and RRab stars are blue. Filled triangles are used for stars for which we detect Blazhko modulations and empty circles are used otherwise. Panel b) displays the Bailey diagram for NGC 5024. The continuous lines represent the average distribution of the RRab and RRC stars in the OoI cluster M3, and the segmented lines are the loci of evolved stars (Cacciari et al. 2005) often seen in OoII clusters like NGC 5024. See Section 6 for a discussion.

the first evidence of modulating non-radial pulsations in three RRC stars in M55. Alcock et al. (2000) reported frequency sidepeaks of main frequency in 2-4% of the RRC variables in the LMC from the MACHO data. Jurcsik et al. (2001) detected amplitude modulations in 8 of 48 RRC stars in ω Cen. According to Piersimoni et al. (2002), the RRC star V48 in NGC 3201 shows amplitude modulations from a single comparison of their light curve amplitude with the amplitude reported by Sawyer-Hogg (1973). However, no evidence is given of an amplitude and/or phase modulated light curve. From the OGLE-I sample, Moskalik & Poretti (2003) identified modulation frequencies in 3 RRC stars in the Galactic bulge (see their Table 8).

In their recent work on M5, Jurcsik et al. (2011) compare period and colour distributions of Blazhko variables and stable RR Lyrae stars. No RRC stars with the Blazhko effect are known in M5. The Blazhko variables discovered in this paper bring the number to 23 confirmed cases among the RRC stars which, to the best of our knowledge, makes NGC 5024 the globular cluster with the largest number of RRC Blazhko variables. Hence, it is of interest to see if the new large population of Blazhko RRC variables in NGC 5024 is consistent with the trends found by Jurcsik et al. (2011) in M5.

Table 4. Detected Blazhko variables in NGC 5024. The main frequency f_0 corresponds to the period reported in Table 2. Under A_m , we list the amplitude of the modulation displayed in the light curves of Figs. 1 and 2. The \mathcal{S}_B statistic is calculated using Eq. 2; in this table we include only stars with $\mathcal{S}_B \geq 145$. In the comments column, we indicate whether the star is located in the “outer” or “inner” region of the cluster and we provide some information on its blend status. All stars in this table are plotted with colour symbols in Figs. 1-4.

Variable	Bailey’s type	f_0 (c/d)	A_m (mag)	\mathcal{S}_B	Comments
V2	RRc	2.589694	0.04	238.5	outer,nb
V4	RRc	2.593300	0.030	662.5	outer,nb
V11 ^a	RRab	1.587438	0.35	3902.3	outer,nb
V15	RRc	3.239475	0.090	283.5	outer, BPix
V16 ^a	RRc	3.298588	0.035	2602.5	outer,nb
V17	RRc	2.623997	0.033	1918.0	outer,nb
V18	RRc	2.975659	0.045	215.8	outer,nb
V23	RRc	2.731188	0.075	2972.7	outer,nb
V25	RRab	1.418132	0.069	148.7	outer,nb
V29	RRab	1.214699	0.038	213.8	outer,nb
V31	RRab	1.417093	0.063	206.6	border,nb
V32	RRc	2.563603	0.057	1692.5	outer,nb
V33	RRab	1.601052	0.02	838.7	outer,blB
V35	RRc	2.683354	0.200	1399.4	outer,nb
V36	RRc	2.678803	0.035	784.4	outer,nb
V38	RRab	1.416846	0.029	210.4	outer,nb
V41	RRab	1.627498	0.143	1165.1	border,nb
V43	RRab	1.404467	0.020	193.4	inner,nb
V44	RRc	2.667321	0.062	369.3	inner,nb
V46	RRab	1.421163	0.037	151.0	inner,nb
V47	RRc	2.981817	0.060	761.2	outer,nb
V51	RRc	2.815196	0.080	529.7	inner, blB
V52 ^b	RRc	2.742574	0.086	1158.3	inner, close to V53
V53 ^b	RRc	2.570166	0.083	677.7	inner, close to V52
V54	RRc	3.173525	0.096	261.9	inner, blB
V55	RRc	2.256180	0.058	913.8	inner,nb
V57 ^a	RRab	1.759807	0.393	2455.7	inner, blB
V58	RRc	2.817132	0.093	351.7	inner, blB
V59	RRc	3.290101	0.077	832.1	inner,bl
V60	RRab	1.550974	0.105	479.2	inner,blB
V61	RRc	2.703214		201.3	inner,bl
V62	RRc	2.778650	0.053	1404.9	inner,nb
V63	RRc	3.220965	0.078	694.6	inner,nb
V64	RRc	3.127698	0.037	311.6	inner,nb

^a Announced as Blazhko variable by Dékány & Kovács (2009), ^b modulations may be an artifact due to proximity with another RR Lyrae
nb: not blended; bl: blended with fainter star; blB: blended with brighter star; Bpix: near to bad pixels

6.1 Trends in brightness, colour and amplitudes of Blazhko variables

Panel (a) of Fig. 7 shows the horizontal branch and the distribution of the Blazhko and stable RR Lyrae stars. There is a clear separation of the RRab and RRc stars indicated by the vertical solid line at $V - I = 0.48$. This has already been noted in Paper I and has been interpreted as the border between the either-or-region (or region where due to hysteresis the first overtone and fundamental pulsators might coexist) (Bono et al. 1997; Szabo et al. 2004) and the fundamental (F) region. The clean separation of fundamental and first overtone pulsators is probably produced when stellar evolution occurs towards the red (Caputo et al. 1978). The two labelled stars, V53 and V60, already noticed and discussed in Paper I, are ignored since they have a peculiar position in the CMD likely due to contamination from a blended star. The RRc stars with Blazhko modulations (filled triangles) in average are redder than the non-modulated stars.

In panel (b) of Fig. 7, we present a Bailey diagram where one

can see that for the RRab stars, the Blazhko and non-Blazhko variables are well mixed, and thus we do not see the trend noticed by Jurcsik et al. (2011) for the case of M5 that Blazhko stars have larger amplitudes and shorter periods. For the RRc stars there is an indication that the Blazhko variables have larger amplitudes and periods but the distribution is very scattered, which is contrary to the trend found in non-modulated stars in M3 or other OoII type clusters (Cacciari et al. 2005). The scatter among the Blazhko RRc stars in NGC 5024 (green triangles in Fig. 7) is most likely connected with amplitude modulations. The dispersion among the non-modulated RRc (green open circles in Fig. 7), of shorter period and smaller amplitude, reminds the equally scattered distribution of the short-period small-amplitude RRc variables V105, V178, and V203 in M3 (see Fig. 2 of Cacciari et al. 2005).

The $V - I$ colour distribution of the RR Lyrae stars in NGC 5024 can also be appreciated in the histogram of Fig. 8. The distribution of the Blazhko RRc variables is redder than that of the stable RRc. This, along with the indication that the evolution is

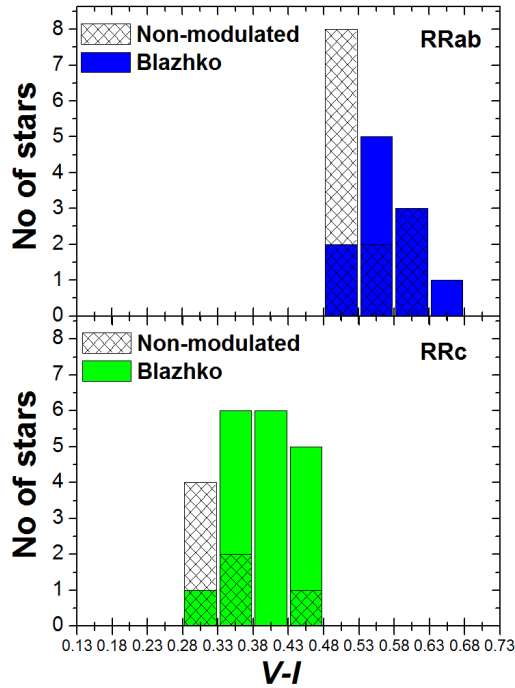


Figure 8. Colour distribution of Blazhko variables (solid colour bars) and non-modulated stars (dashed bars). In average the Blazhko RRc stars are redder than their stable counterparts and tend occupy the either-or or hysteresis region, just to the blue of the fundamental pulsators region. Star V53 and V60 labeled in panel a of Fig. 7 are not considered.

Table 5. RR Lyrae stars classified as non-modulated on the basis of the S_B statistic ($S_B < 145$). Despite of having a low value of S_B , in Figs. 1-4 we have plotted in colour those stars whose light curves display apparent amplitude modulations.

Variable	Bailey's type	S_B -index	Comments
V1	RRab	56.43	outer,nb
V3	RRab	36.7	outer,nb
V5	RRab	78.0	outer,nb
V6	RRab	38.7	outer,nb
V7	RRab	34.5	outer,nb
V8	RRab	39.3	outer,nb
V9	RRab	122.7	outer,nb
V10	RRab	51.1	outer,nb
V19 ^a	RRc	97.0	outer,nb
V24	RRab	48.4	outer,nb
V27	RRab	68.7	outer,nb
V34 ^a	RRc	119.6	outer,nb
V37	RRab	74.0	border,nb
V40 ^a	RRc	43.8	outer,nb
V42 ^a	RRab	51.5	border,nb
V45 ^a	RRab	131.6	inner,nb
V56 ^a	RRc	126.4	inner,nb
V71 ^a	RRc	79.6	inner,blB
V72 ^a	RRc	122.7	inner,nb
V91 ^a	RRc	107.7	inner,nb
V92 ^a	RRc	90.8	inner,nb

^a suspected of amplitude modulations and plotted in colour in Figs. 1-4; nb: not blended; blB: blended with brighter star

towards the red, may suggest that the Blazhko effect manifest systematically in stars undergoing a change in pulsation mode.

6.2 Times of maximum brightness

The times of maximum brightness in a variable star are of fundamental importance since a long record of them help to trace evolutionary changes in the star. In the case of Blazhko variables the variations of the maximum light bear information on the periodicity of the modulation cycle and help to trace the long term variations of the cycle. Dense records of times of maximum is challenging as it requires extensive timely observations. With the conviction that in the future the Blazhko variables in NGC 5024 will be further observed and studied, we measured as many times of maximum light as it has been possible in the light curves of Figs. 1 and 2 and have kept a record of them in Table 6, of which only a small portion is given in the printed version of this paper but the full table is available in electronic form. We have been able to measure between 5 and 11 times of maximum light per star for the majority of the stars. Since the time distribution of our data set is rather limited, we have refrain from attempting a determination of the periodicity in these times of maximum light, but we trust that they will be useful in the future.

In the upper panels of Fig. 9, the phase variations are shown for a group of selected stars with well determined times of maximum light. If the phases on the vertical axis are multiplied by the pulsation period, these plots correspond to the $O - C$ diagrams showing the period variations produced by the Blazhko modulations. The bottom panels display the "loop" diagrams which show the correlation between the amplitude and phase modulations. In cases of continuous dense observations of Blazhko variables (e.g. Guggenberger et al. 2011; Chadid et al. 2010a,b) these plots show loops that indicate whether or not the amplitude and phase modulations are taking place in phase with each other. In our case, despite the sparseness of the Blazhko phase coverage, the plots show general trends between the maximum brightness and phase modulations; we note that for some stars the diagrams display clear traces of the loops (e.g. V11, V57, V23) whereas some others show mild linear trends (V44) or phase variations at constant maximum brightness (V17, V18, V62).

7 CONCLUSIONS

Precise, dense, and long time-span time-series photometry is required to detect amplitude and phase modulations in RR Lyrae variables. If this is achieved, then one may find that the Blazhko effect is more common than generally realized, particularly among the first overtone pulsators or RRc stars. The significant increase in the detections of Blazhko variables in NGC 5024 is mainly due to the high quality of the CCD photometry achieved using the DIA technique which enables one to detect small amplitude and phase modulations. The accuracy of our V photometry at the brightness of the RR Lyrae stars is about 0.008 mag per data point, which is, in most of the confirmed Blazhko variables, significantly smaller than the amplitude of the modulations in the light curves.

Our data reveal that amplitude and phase modulations are present in the majority of the light curves of the RRc stars (23 of 31) and in about half of the RRab stars (11 of 24) in NGC 5024, i.e. 66% and 37% respectively. We also find a lower limit of 52% on the overall incidence rate of the Blazhko effect among the RR

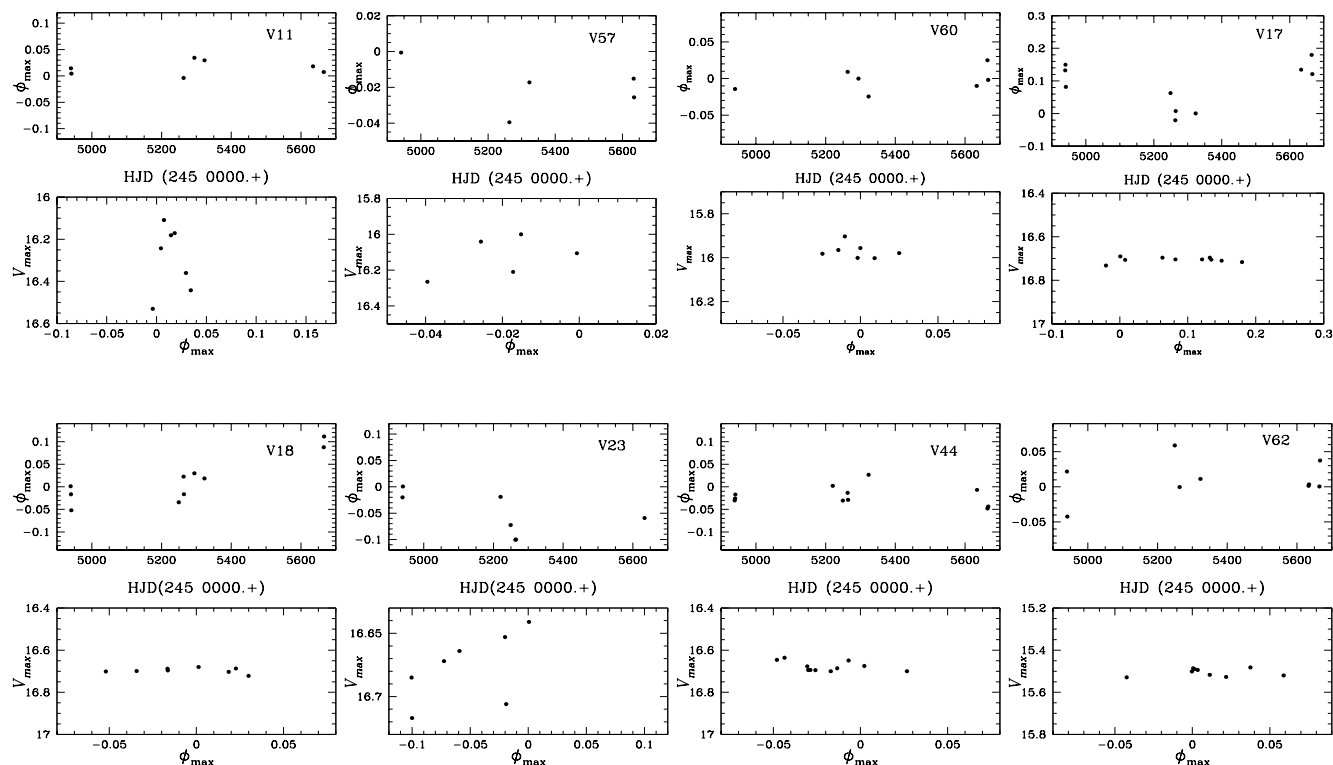


Figure 9. Phase and maximum brightness modulations in for three selected R Rab stars, V11, V57 and V60 and five R R c stars V17, V18, V23, V44, V62.

Table 6. Phase and magnitude at the time of maximum brightness in the V -band for a group of stars with Blazhko modulations. The phase in column 2 was calculated using the ephemerides given in Table 2. This is an extract from the full table, which is available with the electronic version of the article (see Supporting Information).

Star	ϕ_{max}	V_{max}	HJD _{max} (245 0000.+)
V2	+0.000	16.656	4940.34212
V2	-0.039	16.690	5249.24358
...
V4	+0.000	16.681	4939.27817
V4	-0.004	16.688	4941.20439
...
V11	+0.014	16.181	4940.20614
V11	+0.004	16.243	4941.45969
...

Lyrae population of the cluster, a fraction which may increase as more extensive time-series CCD photometry becomes available.

It is likely times of maximum O-C residuals observed in Blazhko variables are caused by the phase modulations. Given the short time base of our observations we cannot say whether or not these O-C differences are at all connected with secular variations in the pulsation period.

The RRab and RRC stars are cleanly separated in the CMD which is the expected situation if the evolution of the RR Lyrae stars is progressing towards the red. In the prevailing hysteresis paradigm, the current pulsation mode of an RR Lyrae star is defined by its previous evolutionary history (e.g., van Albada & Baker 1973; Caputo et al. 1978). As schematically shown in Fig. 3 of Caputo et al. (1978), one only expects to find a clean separation between RRab and RRC stars if horizontal branch evolution is pre-

dominantly towards the red in the instability strip. At the same time, the color distribution of the Blazhko RRC variables is redder than that of the stable counterparts, and populate the hysteresis region where first overtone and fundamental pulsators may coexist. This may suggest that the Blazhko effect manifests in stars undergoing a pulsation mode change.

Our limited time coverage of the Blazhko cycle prevented us from estimating the modulation periods. Despite of this the light curve modulations could be detected with confidence. A continued monitoring of NGC 5024 should prove useful in characterizing the modulation properties of the confirmed and suspected Blazhko stars, in particular the determination of the modulation frequencies. The large sample of Blazhko variables in NGC 5024 will eventually be used to confirm the existence of the correlation between the main pulsation frequency f_0 and the modulation frequency f_m , sketched

for the Blazhko RRab stars in M5 (Jurcsik et al. 2011) and whether the zero point is metallicity dependent. Comprehensive studies of the Blazhko-modulated stars in globular clusters might enable us to study metallicity and stellar evolution effects in RR Lyrae stars and infer incidence rates of the Blazhko modulation in homogeneous populations.

ACKNOWLEDGMENTS

We are grateful to the referee for multiple constructive comments and suggestions. AAF is thankful to the Indian Institute of Astrophysics for hospitality during his sabbatical leave in 2010 and acknowledges support of CONACyT (Mexico), DST (India) and from DGAPA-UNAM through grant IN114309. This work has made a large use of the SIMBAD and ADS services.

REFERENCES

- Alard C., Lupton R.H., 1998, *ApJ*, 503, 325
 Alard C., 2000, *A&AS*, 144, 363
 Alcock C., Allsman R., Alves D. R., Axelrod T., Becker A. and 24 authors, 2000, *ApJ*, 542, 257.
 Arellano Ferro A., Figuera Jaimes R., Giridhar S., Bramich D.M., Hernández J.V., Kuppuswamy K., 2011, *MNRAS*, 416, 2265 (Paper I)
 Benkő J. M., Kolenberg K., Szabó R., Kurtz D. W., Bryson S., and 16 coauthors, 2010, *MNRAS*, 409, 1585
 Benkő J. M., Szabó R., Paparó M., 2011, *MNRAS*, 417, 974
 Blažko, S., *Astron. Nachr.*, 175, 325
 Bono G., Caputo F., Castellani V., Marconi, M., 1997, *A&AS*, 121, 327
 Blu T., Thévenaz P., Unser M., 2001, *IEEE Trans. Image Process.*, 10, 1069
 Bramich D. M., Horne K., Bond I. A., Street R. A., Cameron A. C., Hood B., Cooke J., James D., Lister, T. A., Mitchell D., Pearson K., Penny A., Quirrenbach A., Safizadeh N., Tsapras Y., 2005, *MNRAS*, 359, 1096
 Bramich D.M., 2008, *MNRAS*, 386, L77
 Burke E.W., Rolland W.W., Boy W.R., 1970, *JRASC*, 64, 353
 Cacciari C., Corwin T.M., Carney B.W., 2005, *AJ*, 129, 267
 Caputo F., Tornambe A., Castellani V., 1978, *A&A*, 67, 107
 Chadid M., Benkő J. M., Szabó R., and 14 coauthors, 2010a, *A&A*, 510, A39
 Chadid M., Vernin J., Mekarnia D., Chapellier E., Trinquet, H., Bono, G., 2010b, *A&A*, 516, 15
 Dékány I., Kovács G. 2009, *A&A*, 507, 803
 Dworetzky M.M., 1983, *MNRAS*, 203, 917
 Guggenberger E., Kolenberg K., Chapellier E., Poretti E., Szabó R., Benkő J. M., Paparó M., 2011, *MNRAS*, 415, 1577
 Jurcsik J., Clement C., Geyer E. H., Domsa I., 2001, *AJ*, 121, 951
 Jurcsik J., Sódor Á., Szeidl B., and 9 authors, 2009, *MNRAS*, 400, 1006
 Jurcsik J., Szeidl B., Clement C., Hurta, Zs., Lovas, M., 2011, *MNRAS*, 411, 1763
 Kolenberg K., Szabó R., Kurtz D. W., and 21 authors, 2010, *ApJ*, 713, 198
 Kolenberg K., Bryson S., Szabó R., and 20 authors, 2011, *MNRAS*, 411, 878
 Moskalik P., Poretti E., 2003, *A&A*, 398, 213
 Olech A., Kaluzny J., Thompson I. B., Pych W., Krzeminski W., Schwarzenberg-Czerny A., 1999, *MNRAS*, 310, 759
 Olech A., Kaluzny J., Thompson I. B., Pych W., Krzeminski W., Schwarzenberg-Czerny A., 2001, *MNRAS*, 321, 420
 Piersimoni A.M., Bono G., Ripepi V., 2002, *AJ*, 124, 1528
 Poretti E., Paparó M., Deleuil M., and 13 authors, 2010, *A&A*, 520, 108
 Szabó R., Kolláth, Z., Buchler J. R., 2004, *A&A*, 425, 627
 Sawyer-Hogg H. 1973, *Publ. David Dunlap Obs.*, 3, No. 6
 Shapley H., 1916, *ApJ*, 43, 217
 Smith H. A., 1981, *PASP*, 93, 721
 Székely P., Jackson R., Kiss L.L., Sztatmáry K., 2006, *PADEU* 17, 127
 Tamuz O., Mazeh T., North, P., 2006, *MNRAS*, 367, 1521
 van Albada T. S., Baker N., 1973, *ApJ*, 185, 477
 Walker A. R., 1994, *AJ*, 108, 555